

PIK3CA and *KRAS* Amplification in Esophageal Adenocarcinoma and their Impact on the Inflammatory Tumor Microenvironment and Prognosis



Ahlem Essakly^{*,2}, Heike Loeser^{*,1,2}, Max Kraemer^{*}, Hakan Alakus^{†,1}, Seung-Hun Chon^{†,1}, Thomas Zander^{‡,1}, Reinhard Buettner^{*}, Axel M. Hillmer^{*}, Christiane J. Bruns[†], Wolfgang Schroeder[†], Florian Gebauer^{†,2} and Alexander Quaas^{*,2}

^{*}Institute of Pathology, University Hospital Cologne, Germany; [†]Department of General, Visceral and Cancer Surgery, University Hospital Cologne, Germany; [‡]Department of Internal Medicine I, University Hospital Cologne, Germany

Abstract

Gene amplifications of *PIK3CA* or *KRAS* induce a downstream activation of the AKT-mTOR or RAF-ERK-pathways. Interactions of the active AKT pathway have been implicated in the inflammatory tumor microenvironment. Nothing is known about these interactions or prognostic power in esophageal adenocarcinoma (EAC). We retrospectively analyzed a large cohort of 685 EAC considering *KRAS* and *PIK3CA* gene amplification using fluorescence *in situ* hybridization (FISH) and immunohistochemistry. These results were correlated with clinical and molecular data as well as the inflammatory tumor microenvironment. Amplifications of *KRAS* were seen in 94 patients (17.1%), *PIK3CA* amplifications in 23 patients (5.0%). *KRAS* amplifications significantly correlated with nodal positive patients and poorer overall survival (OS) in the subgroup without neoadjuvant treatment ($p = 0.004$), coamplifications of *Her2* ($p = 0.027$), and *TP53* mutations ($p = 0.016$). *PIK3CA* amplifications significantly correlated with a high amount of tumor infiltrating T cells ($p = 0.003$) and showed a tendency to better OS ($p = 0.068$). A correlation with checkpoint makers (PD-L1, LAG3, VISTA, TIM3, IDO) could not be revealed. Our findings are the first to link the *KRAS* amplified genotype with lymphonodal positivity and poor prognosis and the *PIK3CA*-amplified genotype with a T cell-rich microenvironment in EAC. Future studies must show whether these two genotype subgroups can be therapeutically influenced. A dual inhibition of MEK and SHP2T could be effective in the subgroup of *KRAS* amplified EACs and an immune checkpoint blockade may prove to be particularly promising in the subgroup of *PIK3CA*-amplified EACs.

Translational Oncology (2020) 13, 157–164

Introduction

Esophageal carcinoma is the eighth most common diagnosed malignoma worldwide [1]. The incidence of esophageal adenocarcinomas (EACs) has increased rapidly mainly in the Western world over the past few decades [2–4]. Most of the adenocarcinomas arise from Barrett metaplasia due to chronic reflux disease followed by an accumulation of different mutations, copy-number variations, and chromothripsis causing genetic instability [5]. Despite improvements in perioperative treatments, the overall survival (OS) of patients with EACs remains poor showing a relative 5-year survival rate of about 20.2%. Among the most common mutations of the EACs are *TP53*, *CDKN2A*, and *ARID1a* [6].

Address all correspondence to: Heike Loeser, MD, Institute of Pathology, Gastrointestinal Cancer Group Cologne (GCGC), University Hospital Cologne, Kerpener Str. 62, 50937 Cologne, Germany. E-mail: heike.loeser@uk-koeln.de

¹Gastrointestinal Cancer Group Cologne (GCGC).

²Contributed equally to the work.

Received 12 June 2019; Revised 22 October 2019; Accepted 25 October 2019

© 2019 The Authors. Published by Elsevier Inc. on behalf of Neoplasia Press, Inc. This is an open access article under the CC BY-NC-ND license (<http://creativecommons.org/licenses/by-nc-nd/4.0/>).

1936-5233/19

<https://doi.org/10.1016/j.tranon.2019.10.013>

Interestingly, these and other mutations can already be detected in histologically inconspicuous Barrett's mucosa without dysplasia. The extent of mutations of a dysplastic Barrett mucosa is similar to that of EAC [7–10]. Another example for very early occurring mutations can be seen for *TP53* and *NOTCH1*, as such mutations are found in normal esophageal squamous cell epithelium in healthy volunteers. The probability of mutation increases with age and the extent of *NOTCH1*-mutations is greater than the expected rate of invasive esophageal squamous cell carcinoma [11].

There is growing evidence that copy-number alterations (CNAs) of the genome are the major pathophysiological differences between Barrett's mucosa and invasive adenocarcinoma of the esophagus [12,13]. The most common single loss-of-heterozygosity CNA seen in Barrett's mucosa is *CDK2NA* [14,15].

Copy-number gains (CNGs) are common in the EAC. According to the TCGA data, considering genomic data of approximately 185 EACs, there are putative CNGs among others in *Her2* (in up to 15%), *VEGFA* (14%), *EGFR* (14%), *MET* (4%), *c-MYC* (22%), *GATA6* (12%), *KRAS* (17%), and *PIK3CA* (18%) (compare <http://cancergenome.nih.gov/>) [16–18].

Activating mutations of *KRAS* and *PIK3CA* (or function-inhibiting genomic alterations of *P TEN*) increase the activity of important growth-promoting cancer pathways (RAS-RAF-ERK pathway or PIK-AKT-mTOR pathway). Various studies have shown that CNG/amplification of *KRAS* and *PIK3CA* lead to an activation of these pathways even without additional activating mutations in the genes themselves. According to the TCGA data and other publications, activating gene mutations and amplifications are exclusive (with rare exceptions) [19–21]. Recently, the therapeutic relevance of a *KRAS* amplification in wild-type (nonmutated) *KRAS* tumors of the upper gastrointestinal tract was highlighted and a therapeutic intervention with a combined inhibition of MEK and SHP2 was discussed [22].

Therapeutic interventions of the activated PIK-AKT pathway have been discussed as well and resistance to cisplatin-containing cytostatic therapy is described in ovarian cancer with amplification of *PIK3CA* mRNA [23].

There are no established findings on the prognostic significance of *KRAS* and *PIK3CA* amplification in primary resected or neoadjuvantly treated EACs and their correlation with the inflammatory tumor microenvironment [24].

In colon carcinoma and non-small-cell lung carcinoma, a relationship to mutations and CNA and specific reactions of the (inflammatory) tumor microenvironment was shown [25–29]. Interactions of the activated PIK-AKT pathway with the inflammatory tumor microenvironment have been shown in the past in other tumor entities like colon or ovarian carcinoma [30,31]. Activation of *AKT* leads to the recruitment of different inflammatory cells including CD8 positive T lymphocytes. This interaction is partly because of activation of the NF-kappaB pathway and activation of cyclooxygenase, leading to formation of prostaglandin E2, which enables its receptor to recruit certain T-cell subpopulations [32,33].

Particularly good response rates to immunotherapy can be found in gastric carcinoma or colon carcinoma in the group of microsatellite-unstable tumors (MSIs), histologically typically associated with a strong inflammation in the tumor microenvironment, but this subtype is very rare in the EAC (1%) [29,34,35].

Nevertheless, we see a high variability in the extent of inflammation in the EACs of our tumor collection, but did not correlate molecular alterations of the carcinoma cells yet [36–39].

Thus we examined whether we find interactions between *PIK3CA* amplifications, leading to activation of the AKT pathway, and the recruitment of T lymphocytes into the tumor microenvironment of EAC. Furthermore, we evaluated the frequency of *KRAS* amplification in EAC. In addition, we analyzed the role of potential tumor escape mechanisms against T-cell recruitment by locally immunosuppressive checkpoint markers such as PD-L1, VISTA, LAG3, TIM3, and IDO. Therefore, we performed fluorescence in situ hybridization (FISH) and immunohistochemistry of 685 EACs, allowing us to accurately determine the extent of gene amplifications on a very large tumor cohort and correlated these results with clinical and additional molecular data and the composition of the inflammatory tumor microenvironment.

Material and Methods

Patients and Tumor Samples

We analyzed formalin-fixed and paraffin-embedded (FFPE) material of 685 patients with EAC in total that underwent primary surgical resection or resection after neoadjuvant therapy between 1999 and 2016 at the Department of General, Visceral and Cancer Surgery, University of Cologne, Germany. The standard surgical procedure consisted of a transthoracic en-bloc esophagectomy with two-field lymphadenectomy (abdominal and mediastinal lymph nodes), reconstruction was done by formation of a gastric tube with intrathoracic esophagogastronomy (Ivor Lewis esophagectomy) [40]. The abdominal phase was predominantly performed as a laparoscopic procedure (hybrid Ivor Lewis esophagectomy). Technical details of this operation are described elsewhere [41–43]. Patients with advanced esophageal cancer (cT3, cNx, M0) received preoperative chemoradiation (5-FU, cisplatin, 40Gy as treated in the area prior the CROSS trial) or chemotherapy alone. The follow-up of all patients was performed according to a standardized protocol. During the first two years, clinical follow-up of patients was performed in the hospital every three months, followed by annual exams. These included clinical evaluation, abdominal ultrasound, chest X-ray, and additional diagnostic procedures as required. Follow-up data were available for all patients. Patient characteristics are given in Table 1. Depending on the effect of neoadjuvant chemo- or radiochemotherapy, there is a preponderance of minor responders in the tissue microarrays (TMAs), defined as histopathological residual tumor of $\geq 10\%$ [44].

All procedures performed in studies involving human participants were in accordance with the ethical standards of the institutional research committee and with the 1964 Helsinki declaration and its later amendments or comparable ethical standards.

TMA Construction

For TMA, one tissue core from each tumor was punched out and transferred into a TMA-recipient block. TMA construction was performed as previously described [45,46]. In brief, tissue cylinders with a diameter of 1.2 mm each were punched from selected tumor tissue blocks using a self-constructed semiautomated precision instrument and embedded in empty recipient paraffin blocks.

Consecutive sections of the resulting TMA blocks were transferred to an adhesive-coated slide system (Instrumedics Inc., Hackensack, NJ) for immunohistochemistry and FISH.

Analysis of Heterogeneity of Amplification

To clarify the important question of the heterogeneous distribution of amplified tumor clones, we further analyzed all amplified tumors

Table 1. Patients' Characteristics, *KRAS* (*n* = 526) and *PIK3CA* (*n* = 461) Amplification Status.

		KRAS				PIK3CA			
		Total	Negative	Amplified	<i>p</i> value	Total	Negative	Amplified	<i>p</i> value
Total		526	432	94		461	437	24	
Sex	Female	100%	82.1%	17.9%	0.719	100%	94.8%	5.5%	0.339
	Male	59	50	9		54	53	1	
Age group	<65 yrs	11.2%	84.7%	15.3%	0.416	11.7%	98.1%	1.9%	0.836
	<65 yrs	467	382	85		407	384	23	
Tumor stage	pT1	88.8%	81.8%	18.2%	0.880	88.3%	94.3%	5.7%	0.217
	pT2	261	217	44		225	212	13	
	pT3	52.6%	83.1%	16.9%		48.8%	94.2%	5.8%	
	pT4	235	188	47		212	201	11	
Lymph node metastasis	pN0	47.4%	80.0%	20.0%	0.004	51.2%	94.8%	5.2%	0.290
	pN+	74	63	11		63	56	7	
UICC stage	I	14.1%	85.1%	14.9%	0.146	13.7%	88.9%	11.1%	0.198
	II	60	49	11		51	48	3	
	III	11.5%	81.7%	18.3%		11.1%	94.1%	5.9%	
	IV	370	302	68		330	317	13	
Her2 status	Wild type	70.6%	81.6%	18.4%	0.027	71.7%	96.1%	3.9%	1.00
	Amplified	18	14	4		14	13	1	
TP53 status	Wild type	3.4%	77.8%	22.2%	0.016	3.0%	92.9%	7.1%	0.812
	Mutation	209	184	25		181	169	12	
UICC stage	I	39.9%	88.0%	12.0%	0.146	39.4%	93.4%	6.6%	0.198
	II	315	246	69		278	266	12	
	III	60.1%	78.1%	21.9%		60.6%	95.7%	4.3%	
	IV	114	99	15		94	85	9	
Her2 status	Wild type	21.8%	86.8%	13.2%	0.027	20.6%	90.4%	9.6%	1.00
	Amplified	114	98	16		106	101	5	
TP53 status	Wild type	21.8%	86.0%	14.0%	0.016	23.2%	95.3%	4.7%	0.812
	Mutation	218	173	45		191	179	12	
UICC stage	I	41.8%	78.4%	21.6%	0.016	42.0%	95.8%	4.2%	0.812
	II	76	60	16		65	63	2	
	III	14.6%	78.9%	21.1%		14.2%	96.9%	3.1%	
	IV	311	252	59		274	256	18	
Her2 status	Wild type	88.1%	81.0%	19.0%	0.027	87.8%	93.4%	6.6%	1.00
	Amplified	42	40	2		38	36	2	
TP53 status	Wild type	11.9%	95.2%	4.8%	0.016	12.2%	94.7%	5.30%	0.812
	Mutation	155	138	17		136	129	7	
UICC stage	I	41.6%	89.0%	11.0%	0.016	41.6%	94.9%	5.10%	0.812
	II	218	173	45		191	179	12	
	III	58.4%	46.4%	12.1%		58.4%	54.7%	3.70%	
	IV	218	173	45		191	179	12	

on large tumor surfaces and constructed a heterogeneity tissue microarray (h-TMA) of 48 tumors. This h-TMA contains each three *KRAS*- and *PIK3CA*-amplified tumors, which were also analyzed on large surfaces, and additional 45 nonamplified tumors. Standard TMAs typically use one biopsy per tumor, whereas the h-TMA takes into account up to 12 biopsies per tumor. In tumors without lymphonodal metastases (*n* = 25) we punched out four biopsies from the tumor surface and four from the infiltration zone of the tumor periphery. In lymphonodal positive tumors (*n* = 23), four additional biopsies were taken from the lymph node biopsies.

Immunohistochemistry

The *KRAS* antibody (clone 9.13, Thermo Fisher, dilution 1:100) and *PIK3CA* antibody (clone 6D9, Thermo Fisher, dilution 1:1000) stainings were performed on TMA slides using the Ventana Benchmark stainer (Roche Diagnostics, Germany) according to the protocol of the manufacturers. Expression of *KRAS* and *PIK3CA* in the cytoplasm of carcinoma cells were assessed according to the following criteria: negative or weak staining in <5% of tumor cells (score 0); weak staining ≥ 5 –20% of tumor cells (score 1); moderate to strong staining in ≥ 20 % (score 2; compare Figure 3). The evaluation of immunohistochemical expression was assessed manually by two pathologists (A.Q. and A.E.). Discrepant results, which occurred in a small number of samples, were resolved by consensus

review. Additional immunohistochemical markers were evaluated in this cohort of EAC, parts of it (*VISTA*, *CD3*) published [39], others (*PD-L1*, *LAG3*, *TIM3*, *IDO*) are currently under review. In brief, monoclonal antibodies were used (Ventana: *PD-L1*; Cell Signaling Technology: *LAG3*, *TIM3*, *IDO*) on the Ventana Benchmark stainer (*PD-L1*) or the Leica *BOND-MAX* stainer (Leica Biosystems, Germany) (*LAG3*, *TIM3*, and *IDO*). The expression in <1% lymphocytes were defined as negative and ≥ 1 % was assessed as positive.

Fluorescence In Situ Hybridization

FISH for the evaluation of the *KRAS* gene amplification status was performed with the Zytolight SPEC *KRAS/CEN12* Dual Color Probe (Zytovision, Germany) according to the manufacturers' protocol. For *PIK3CA* gene amplification analysis, the Zytolight SPEC *PIK3CA/CEN3* Dual Probe Kit (Zytovision, Germany) was used according to the manufacturers' protocol. Sample processing was performed as described previously [47]. Tumor tissue was scanned for gene copy gains including chromosomal cluster amplifications hot spots using a 63 \times objective (DM5500 fluorescent microscope; Leica, Germany). In case the signals were homogeneously distributed, then random areas were used for counting the signals. Twenty tumor cells were evaluated by counting green *KRAS* or *PIK3CA* and orange centromere signals. The reading strategy for detecting amplifications

followed the recommendations *KRAS/CEN12* ratio >3.0 or *KRAS* extrachromosomal cluster amplifications signals [48]. For *PIK3CA* reading strategy followed the recommendations of previous studies *PIK3CA/CEN3* ratio ≥ 2.0 or *PIK3CA* signals ≥ 5.0 proof an amplification [49,50].

Statistical Analysis

Clinical data were collected prospectively according to a standardized protocol. For statistical analysis, SPSS Statistics for Mac (Version 21, SPSS) was used. Interdependence between staining and clinical data was calculated using the chi-squared and Fisher's exact tests and displayed by cross tables. Survival curves were plotted using the Kaplan–Meier method and analyzed using the log-rank test.

Results

Clinicopathological and Patients' Characteristics

The entire cohort consisted of 685 patients with EAC were considered for analysis, in total there were 526 analyzable cases for *KRAS* (76.2%) and 461 cases for *PIK3CA* (67.3%) on the TMA. Reasons for noninformative cases included lack of tissue samples or absence of unequivocal cancer tissue in the TMA spot. Neoadjuvant treatment (either chemoradiation or chemotherapy) was administered in 403 patients (58.5%). The median follow-up for the entire cohort was 57.7 months with a calculated 5-year survival rate of 26.6% (compare Table 1 with patients' and tumor characteristics).

KRAS Amplification Status

KRAS amplifications were seen in 94 patients (17.1%). The amplification profile was not affected by administration of neoadjuvant treatment. Within the group of patients that underwent primary surgery, 41 patients showed *KRAS* amplification (18.1%) and 52 patients (17.7%) in the group of neoadjuvant treatment and resection ($p = 0.909$).

KRAS amplifications were not associated with sex ($p = 0.719$), patient's age ($p = 0.416$), and tumor stage ($p = 0.880$). Nodal positive patients (pN+) significantly correlated with a higher frequency of *KRAS* amplification ($p = 0.004$; Table 1). We found a correlation between *KRAS* amplification and *Her2* amplifications ($p = 0.027$) and *TP53* mutations ($p = 0.016$), respectively. A correlation between the inflammatory tumor microenvironment (CD3 positive T-cells, PD-L1, LAG3, VISTA, TIM3, IDO expression) could not be found.

PIK3CA Amplification Status

PIK3CA amplifications were seen in 23 patients (5.0%). Similar amplification rates were seen within the primary surgery group ($n = 10$; 4.9%) and surgery after neoadjuvant treatment ($n = 13$; 5.1%) ($p = 1.000$).

PIK3CA amplifications showed no correlation with sex ($p = 0.501$), patient's age ($p = 0.673$), tumor stage ($p = 0.155$), lymph node metastasis ($p = 0.669$), *Her2* amplifications ($p = 0.488$), or *TP53* mutations ($p = 0.132$). In tumors with a high amount of tumor infiltrating T cells (CD3 high), the frequency of *PIK3CA* amplifications was significantly higher (11.9%) compared with T-cell low tumors (3.0%, $p = 0.003$) (compare Figure 1). A correlation with any of the analyzed immune checkpoint makers (PD-L1, LAG3, VISTA, TIM3, IDO) could not be revealed.

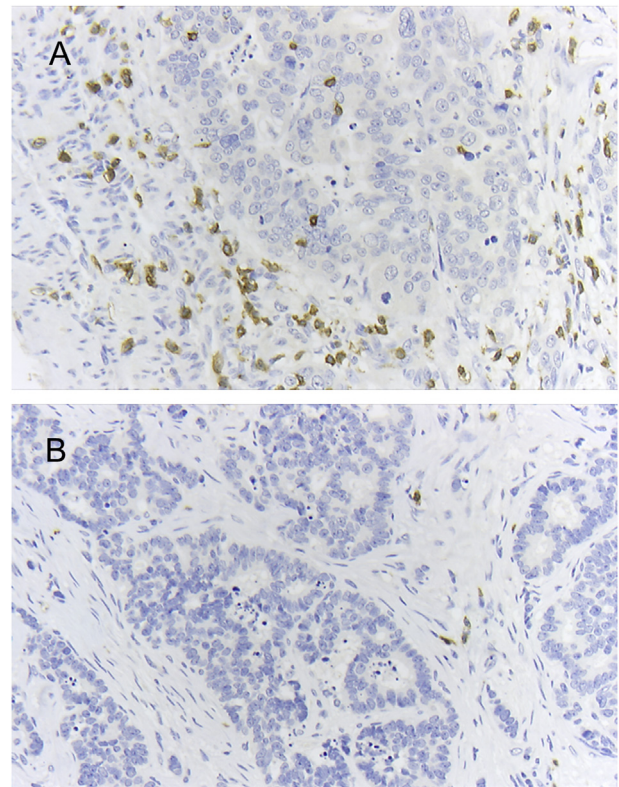


Figure 1. Esophageal adenocarcinoma showing (A) high amounts of tumor infiltrating CD3-positive T cells (brown cells) and (B) low content of CD3-positive T cells; magnification $\times 200$.

KRAS and *PIK3CA* and Prognosis

Survival analysis on the entire patients' cohort did not show any difference in OS in dependence on the *KRAS* status (Figure 2). However, when analyzing the patient group with primary resection, there was a significant survival difference with a worse outcome for patients with *KRAS* amplifications. The median OS for *KRAS* nonamplified patients was 64.9 months (95% confidence interval (95%CI) 29.3–100.4 months) and for amplified patients 16.2 months (95%CI, 1.2–39.5 months, $p = 0.050$). For *PIK3CA*, no difference in OS was detectable for the entire patients' group ($p = 0.830$). Stratifying patients with and without neoadjuvant treatment did not reach a statistical significance. In patients without neoadjuvant treatment, median OS was 202.2 months (95% not achieved) compared with a median OS of 45.7 months (95% CI 26.2–65.2 months, $p = 0.068$).

A multivariate cox proportional hazard model revealed the presence of lymph node metastases as an independent prognostic marker ($p < 0.001$), but not *KRAS* or *PIK3CA* amplifications (Table 2).

Heterogeneity of Amplification

In *KRAS*, 15 amplified tumors showed homogeneous amplification across the tumor (both on the large tumor surface and on the h-TMA spots) and all nonamplified tumors were confirmed. In *PIK3CA*, three of the nine amplified tumors showed a heterogeneous distribution of the amplified tumor clones.

The heterogeneous distribution of *PIK3CA* also affects two cases with lymph node metastases that have both amplified and nonamplified tumor clones within the metastases.

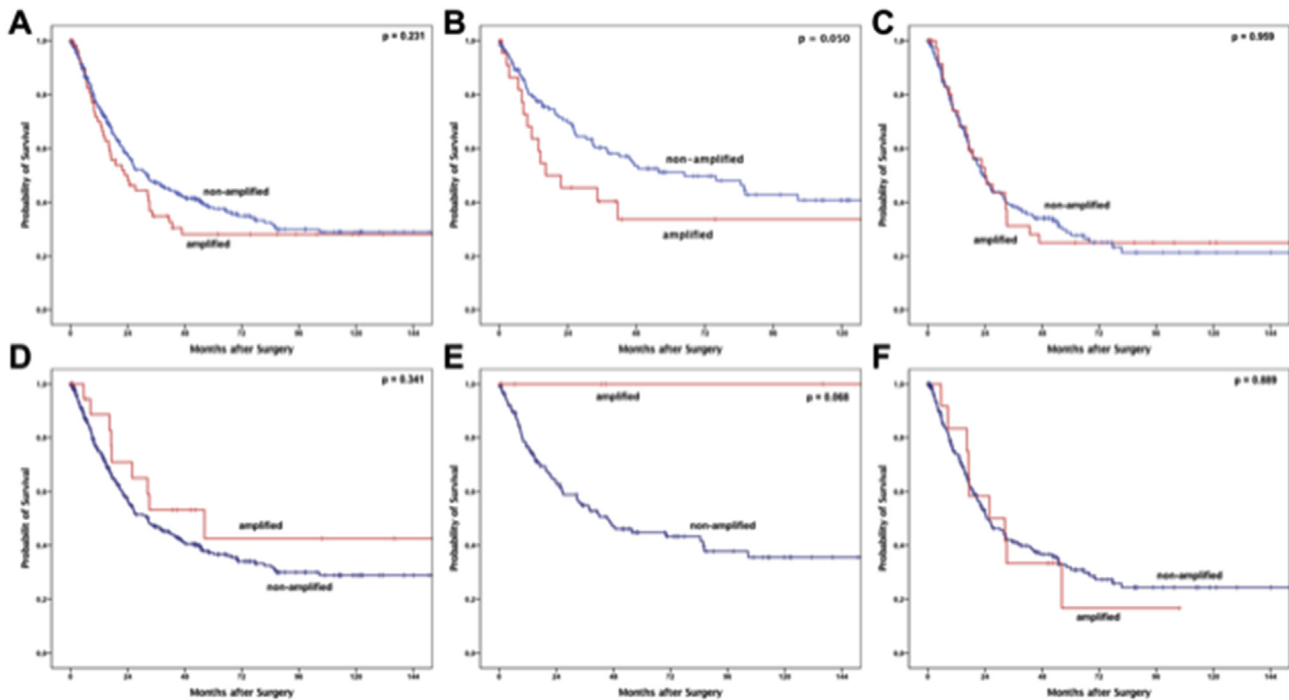


Figure 2. Overall survival using Kaplan–Meier analyses; (A) *KRAS* amplification for the entire patients cohort, (B) patients with primary surgery, and (C) patients with neoadjuvant treatment before operation; (D) *PIK3CA* amplification for the entire patients cohort, (E) patients with primary surgery, and (F) patients after neoadjuvant treatment.

Immunohistochemistry

All tumors that harbored *KRAS* and *PIK3CA* amplifications also expressed *KRAS* and *PIK3CA* protein visualized by immunohistochemistry (Figure 3).

Discussion

We found higher amplification rates for *KRAS* in our large tumor population than were reported in the TCGA cohort for adenocarcinoma of the esophagus [16,17], but confirm data from a recently published large study including tumors of the gastroesophageal junction [19].

To describe copy-number variations, differently suitable techniques can be used. FISH analysis allows us to precisely characterize the CNGs in tumor cells. FISH analysis is actually the current standard technique for evaluation of single-gene amplifications. We defined *KRAS* amplification according to internationally accepted criteria as a ratio of >3 and correlated our gene amplification results with protein expression of *KRAS*, which we determined by immunohistochemistry. We have found an excellent concordance between gene amplification and protein expression (Figure 3) and can confirm the results of a previous study describing the same concordance [19].

We were able to show that *KRAS* amplified tumors represent a more aggressive subset of tumors in the primary resected, non-neoadjuvantly treated EACs mainly driven by the accumulation of lymph node metastases in this group.

This effect was no longer measurable in the neoadjuvant-treated group (combined radiochemotherapy according to the CROSS scheme or chemotherapy according to the FLOT scheme).

This is probably because of the already very unfavorable starting situation with higher clinical tumor stages and neoadjuvant pretreated pathohistological minor responders (= tumors which have an inadequate response rate with ≥10% vital tumor proportion) [44,51]. The minor responders are enriched in our collection of pretreated EACs, as in the prognostically more favorable complete responders no vital tumor is detectable in the surgical specimens, thus no tumor is present for further analyses.

In the cohort of EAC, we see no difference of *KRAS* amplification rates correlating the primary resected and the neoadjuvant subgroup, indicating no influence of neoadjuvant therapy concepts on the rate of *KRAS* amplifications.

We interpret the homogeneity of *KRAS* amplification as a signal of the biological relevance of this gene multiplication, probably underlining the high therapeutic effectiveness of pathway inhibition in these tumors.

In our collection, we observe an accumulation of *TP53* mutated and *KRAS*-amplified tumors as well as coamplifications of *Her2* and *KRAS*. Future studies will need to demonstrate whether personalized therapy with combinatorial inhibition of MEK and SHP2 is effective in the subset of *KRAS* amplified EACs as discussed most recently [19]. We do not see any impact on the inflammatory tumor microenvironment in *KRAS* amplified tumors.

PIK3CA amplification occurs less frequently than *KRAS* amplification in EACs. Primary resected patients with *PIK3CA* amplifications

Table 2. Multivariate Cox-Regression Model.

	Hazard Ratio	95% Confidence Interval		p value
		Lower	Upper	
Sex	1.649	0.891	3.051	0.111
Age group (<65 vs. > 65 years)	1.249	0.925	1.686	0.146
Tumor stage (pT1/2 vs. pT3/4)	1.359	0.856	2.156	0.193
Lymph node metastasis (pN0 vs. pN+)	3.595	2.48	5.211	<0.001
<i>KRAS</i> (amplified vs. nonamplified)	0.83	0.567	1.217	0.341
<i>PIK3CA</i> (amplified vs. nonamplified)	0.924	0.482	1.771	0.811

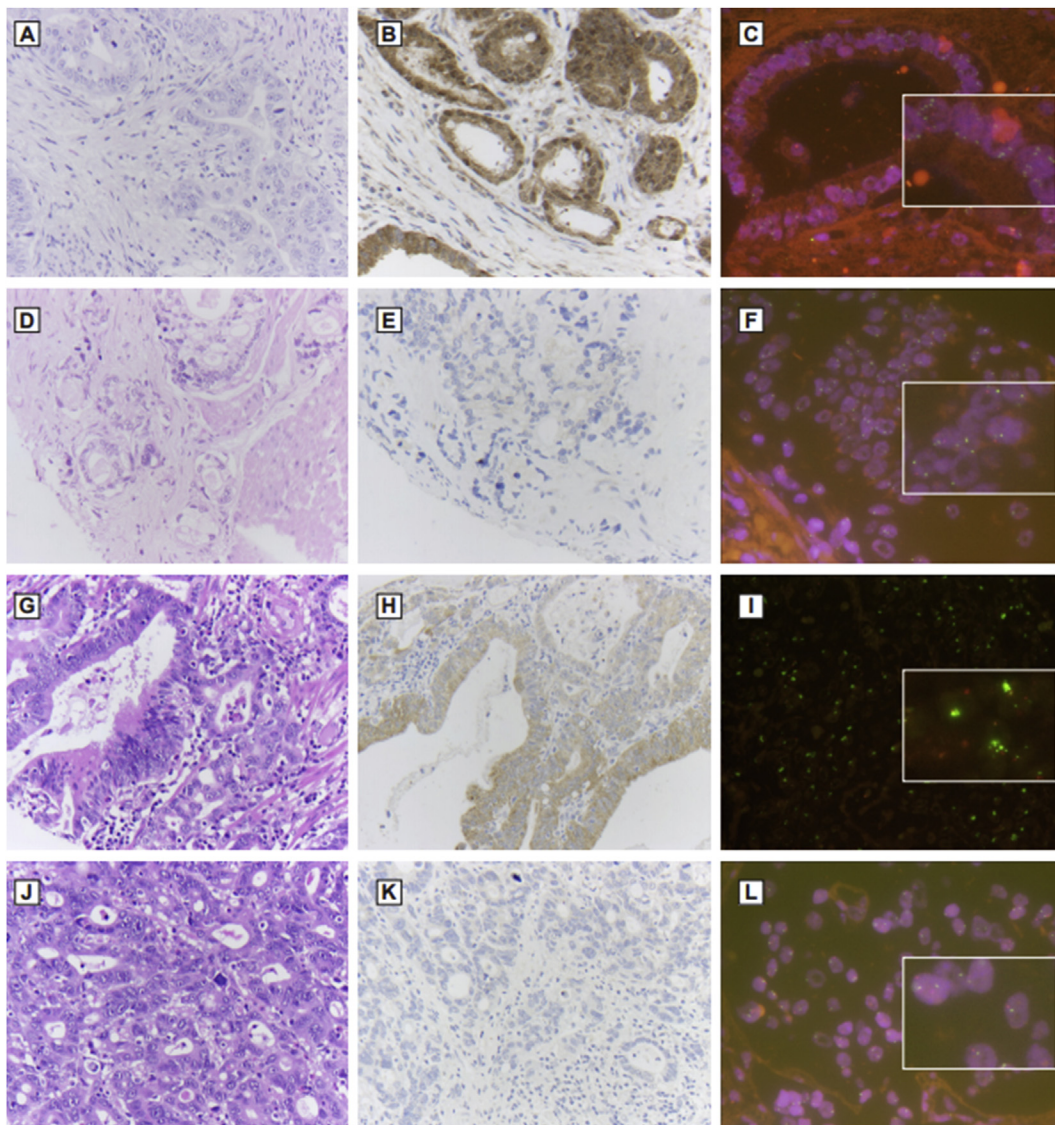


Figure 3. KRAS and PIK3CA gene amplification and protein expression, magnification x200. (A–C) PIK3CA positive: (A) esophageal adenocarcinoma (HE), (B) PIK3CA immunohistochemistry shows strong expression of the protein within the tumor, (C) *PIK3CA* amplification via FISH (red signals: centromere 3, green signals: *PIK3CA* gene). (D–E) PIK3CA negative: (D) Esophageal adenocarcinoma (HE), (E) PIK3CA immunohistochemistry shows no expression of the protein within the tumor, (F) *PIK3CA* nonamplified tumor via FISH with normal signal distribution pattern. (G–I) KRAS positive: (G) esophageal adenocarcinoma (HE), (H) KRAS immunohistochemistry shows strong expression of the protein within the tumor, (I) *KRAS* amplification via FISH (red signals: centromere 12, green signals: *KRAS* gene region with clusters). (J–L) KRAS negative: (J) Esophageal adenocarcinoma (HE), (K) KRAS immunohistochemistry shows no expression of the protein within the tumor, (L) *KRAS* nonamplified tumor via FISH with normal signal distribution pattern.

show a favorable prognosis; however, statistical significance is not achieved ($p = 0.068$). Conflicting results are found in the literature in esophageal squamous cell carcinoma. One work finds an unfavorable prognosis in *PIK3CA* amplifications, another study shows a favorable prognosis in activating *PIK3CA* mutations [52,53]. To our knowledge, nothing is known about the prognostic significance of *PIK3CA* amplification in EAC. A study on gastric carcinoma in Asian patients showed an unfavorable prognosis and a very high percentage of more than 60% *PIK3CA*-amplified gastric tumors [24]. Considering the inflammatory tumor environment, *PIK3CA*-amplified tumors have a significant accumulation of T lymphocytes. We observed in our tumor collection (data not published), as well as other studies, a favorable prognosis of T cell–rich inflammation in EAC [36–38].

The T-cell enrichment in the microenvironment may explain the tendency to the favorable prognosis of *PIK3CA*-amplified EACs.

This interesting relationship between gene amplification, tumor cell–associated cancer pathway activation, and effect on the inflammatory tumor microenvironment could be explained by the PIK-AKT pathway–mediated activation of the NF-kappaB pathway, as previously described on colitis-associated colon carcinoma or on ovarian carcinoma [30,31]. The activation of AKT is linked to an accumulation of inflammatory cells in the tumor microenvironment such as CD8 + T lymphocytes, whereas cyclooxygenase 2, which is also typically found on activation of this pathway, can regulate the synthesis of prostaglandin E₂ (PEG₂) leading to an accumulation of certain T cells via its PEG₂ receptor [32,33]. Because a T cell–rich

tumor microenvironment may be detrimental to the survival of the tumor, it is useful to establish escape mechanisms against T-cell inflammation. The upregulation of specific immunosuppressive checkpoint markers such as PD-L1, LAG3, IDO, TIM3, and VISTA may be helpful.

Therefore, we examined these checkpoint markers in our tumor population, but see no relation of an accumulation of these checkpoint markers and T cell-rich tumors with amplification of *PIK3CA*. Apparently, T cell-rich *PIK3CA*-amplified tumors are a subtype of EAC choosing other strategies of immune escape. Further studies need to clarify the interactions of copy-number variations and the tumor microenvironment.

Possible limitations of our work are the retrospective nature of the analyzes, the restriction to surgical specimens, and the accumulation of minor responders in our group of neoadjuvant-treated patients. Statements on the distribution of *KRAS*- or *PIK3CA*-amplified tumors in nonpretreated biopsy specimens and correlation to complete responders after neoadjuvance cannot be made.

Conclusions

In conclusion, this work on a very large collection of EAC shows that *KRAS* amplification is prognostically unfavorable in primary resected EACs, whereas the *PIK3CA*-amplified genotype with T cell-rich inflammatory tumor microenvironment shows a tendency to a better OS.

Future studies must show to what extent these two different tumor subgroups can be therapeutically influenced in the EAC. Thus, in the subgroup of *KRAS*-amplified EACs a dual inhibition of MEK and SHP2 and in the subgroup of *PIK3CA*-amplified EACs an immune checkpoint blockade may prove to be particularly promising.

Funding

Max Kraemer was supported by the Koeln Fortune Program/Faculty of Medicine, University of Cologne, grant number 410/2018.

Declarations of Interest

None.

Appendix A. Supplementary data

Supplementary data to this article can be found online at <https://doi.org/10.1016/j.tranon.2019.10.013>.

References

- [1] Enzinger PC and Mayer RJ (2003). Esophageal cancer. *N Engl J Med* **349**(23), 2241–2252.
- [2] Lepage C, Rachet B, Jooste V, Faivre J and Coleman MP (2008). Continuing rapid increase in esophageal adenocarcinoma in England and Wales. *Am J Gastroenterol* **103**(11), 2694–2699.
- [3] Edgren G, Adami HO, Weiderpass E and Nyren O (2013). A global assessment of the oesophageal adenocarcinoma epidemic. *Gut* **62**(10), 1406–1414.
- [4] Pohl H, Sirovich B and Welch HG (2010). Esophageal adenocarcinoma incidence: are we reaching the peak? *Cancer Epidemiol Biomarkers Prev* **19**(6), 1468–1470.
- [5] Barrett JC (1993). Mechanisms of multistep carcinogenesis and carcinogen risk assessment. *Environ Health Perspect* **100**, 9–20.
- [6] Frankell AM, Jammula S, Li X, Contino G, Killcoyne S, Abbas S, Perner J, Bower L, Devonshire G and Ococks E, et al (2019). The landscape of selection in 551 esophageal adenocarcinomas defines genomic biomarkers for the clinic. *Nat Genet* **51**(3), 506–516.
- [7] Prevo LJ, Sanchez CA, Galipeau PC and Reid BJ (1999). p53-mutant clones and field effects in Barrett's esophagus. *Cancer Res* **59**(19), 4784–4787.
- [8] Contino G, Vaughan TL, Whiteman D and Fitzgerald RC (2017). The Evolving Genomic Landscape of Barrett's Esophagus and Esophageal Adenocarcinoma. *Gastroenterology* **153**(3), 657–673. e1.
- [9] Agrawal N, Jiao Y, Bettgowda C, Hutfless SM, Wang Y, David S, Cheng Y, Twaddell WS, Latt NL and Shin EJ, et al (2012). Comparative genomic analysis of esophageal adenocarcinoma and squamous cell carcinoma. *Cancer Discov* **2**(10), 899–905.
- [10] Weaver MJ, Ross-Innes CS, Shannon N, Lynch AG, Forshew T, Barbera M, Murtaza M, Ong CJ, Lao-Siriex P and Dunning MJ, et al (2014). Ordering of mutations in preinvasive disease stages of esophageal carcinogenesis. *Nat Genet* **46**(8), 837–843.
- [11] Martincorena I, Fowler JC, Wabik A, Lawson ARJ, Abascal F, Hall MWJ, Cagan A, Murai K, Mahbubani K and Stratton MR, et al (2018). Somatic mutant clones colonize the human esophagus with age. *Science* **362**(6417), 911–917.
- [12] Secrier M, Li X, de Silva N, Eldridge MD, Contino G, Bornschein J, MacRae S, Grehan N, O'Donovan M and Miremadi A, et al (2016). Mutational signatures in esophageal adenocarcinoma define etiologically distinct subgroups with therapeutic relevance. *Nat Genet* **48**(10), 1131–1141.
- [13] Nones K, Waddell N, Wayte N, Patch AM, Bailey P, Newell F, Holmes O, Fink JL, Quinn MCJ and Tang YH, et al (2014). Genomic catastrophes frequently arise in esophageal adenocarcinoma and drive tumorigenesis. *Nat Commun* **5**, 5224.
- [14] Ross-Innes CS, Becq J, Warren A, Cheetham RK, Northen H, O'Donovan M, Malhotra S, di Pietro M, Ivakhno S and He M, et al (2015). Whole-genome sequencing provides new insights into the clonal architecture of Barrett's esophagus and esophageal adenocarcinoma. *Nat Genet* **47**(9), 1038–1046.
- [15] Galipeau PC, Prevo LJ, Sanchez CA, Longton GM and Reid BJ (1999). Clonal expansion and loss of heterozygosity at chromosomes 9p and 17p in premalignant esophageal (Barrett's) tissue. *J Natl Cancer Inst* **91**(24), 2087–2095.
- [16] Gao J, Aksoy BA, Dogrusoz U, Dresdner G, Gross B, Sumer SO, Sun Y, Jacobsen A, Sinha R and Larsson E, et al (2013). Integrative analysis of complex cancer genomics and clinical profiles using the cBioPortal. *Sci Signal* **6**(269), p11.
- [17] Chen Y, McGee J, Chen X, Doman TN, Gong X, Zhang Y, Hamm N, Ma X, Higgs RE and Bhagwat SV, et al (2014). Identification of druggable cancer driver genes amplified across TCGA datasets. *PLoS One* **9**(5), e98293.
- [18] Das K, Gunasegaran B, Tan IB, Deng N, Lim KH and Tan P (2014). Mutually exclusive FGFR2, HER2, and KRAS gene amplifications in gastric cancer revealed by multicolour FISH. *Cancer Lett* **353**(2), 167–175.
- [19] Wong GS, Zhou J, Liu JB, Wu Z, Xu X, Li T, Xu D, Schumacher SE, Puschhof J and McFarland J, et al (2018). Targeting wild-type KRAS-amplified gastroesophageal cancer through combined MEK and SHP2 inhibition. *Nat Med* **24**(7), 968–977.
- [20] Mekenkamp LJ, Tol J, Dijkstra JR, de Krijger I, Vink-Borger ME, van Vliet S, Teerenstra S, Kamping E, Verwiel E and Koopman M, et al (2012). Beyond KRAS mutation status: influence of KRAS copy number status and microRNAs on clinical outcome to cetuximab in metastatic colorectal cancer patients. *BMC Cancer* **12**, 292.
- [21] Mita H, Toyota M, Aoki F, Akashi H, Maruyama R, Sasaki Y, Suzuki H, Idogawa M, Kashima L and Yanagihara K, et al (2009). A novel method, digital genome scanning detects KRAS gene amplification in gastric cancers: involvement of overexpressed wild-type KRAS in downstream signaling and cancer cell growth. *BMC Cancer* **9**, 198.
- [22] Courtney KD, Corcoran RB and Engelman JA (2010). The PI3K pathway as drug target in human cancer. *J Clin Oncol* **28**(6), 1075–1083.
- [23] Lee S, Choi EJ, Jin C and Kim DH (2005). Activation of PI3K/Akt pathway by PTEN reduction and PIK3CA mRNA amplification contributes to cisplatin resistance in an ovarian cancer cell line. *Gynecol Oncol* **97**(1), 26–34.
- [24] Shi J, Yao D, Liu W, Wang N, Lv H, Zhang G, Ji M, Xu L, He N and Shi B, et al (2012). Highly frequent PIK3CA amplification is associated with poor prognosis in gastric cancer. *BMC Cancer* **12**, 50.
- [25] Herbst RS, Morgensztern D and Boshoff C (2018). The biology and management of non-small cell lung cancer. *Nature* **553**(7689), 446–454.
- [26] Le DT, Uram JN, Wang H, Bartlett BR, Kemberling H, Eyring AD, Skora AD, Lubner BS, Azad NS and Laheru D, et al (2015). PD-1 Blockade in Tumors with Mismatch-Repair Deficiency. *N Engl J Med* **372**(26), 2509–2520.

- [27] Koyama S, Akbay EA, Li YY, Aref AR, Skoulidis F, Herter-Sprie GS, Buczkowski KA, Liu Y, Awad MM and Denning WL, et al (2016). STK11/LKB1 Deficiency Promotes Neutrophil Recruitment and Proinflammatory Cytokine Production to Suppress T-cell Activity in the Lung Tumor Microenvironment. *Cancer Res* **76**(5), 999–1008.
- [28] Vermeulen L, De Sousa EMF, van der Heijden M, Cameron K, de Jong JH, Borovski T, Tuynman JB, Todaro M, Merz C and Rodermond H, et al (2010). Wnt activity defines colon cancer stem cells and is regulated by the microenvironment. *Nat Cell Biol* **12**(5), 468–476.
- [29] Llosa NJ, Cruise M, Tam A, Wicks EC, Hechenbleikner EM, Taube JM, Blosser RL, Fan H, Wang H and Lubber BS, et al (2015). The vigorous immune microenvironment of microsatellite instable colon cancer is balanced by multiple counter-inhibitory checkpoints. *Cancer Discov* **5**(1), 43–51.
- [30] Sun Y, Zhao Y, Wang X, Zhao L, Li W, Ding Y, Kong L, Guo Q and Lu N (2016). Wogonoside prevents colitis-associated colorectal carcinogenesis and colon cancer progression in inflammation-related microenvironment via inhibiting NF-kappaB activation through PI3K/Akt pathway. *Oncotarget* **7**(23), 34300–34315.
- [31] Yang N, Huang J, Greshock J, Liang S, Barchetti A, Hasegawa K, Kim S, Giannakakis A, Li C and O'Brien-Jenkins A, et al (2008). Transcriptional regulation of PIK3CA oncogene by NF-kappaB in ovarian cancer microenvironment. *PLoS One* **3**(3), e1758.
- [32] Ricciotti E and FitzGerald GA (2011). Prostaglandins and inflammation. *Arterioscler Thromb Vasc Biol* **31**(5), 986–1000.
- [33] Weichhart T and Saemann MD (2008). The PI3K/Akt/mTOR pathway in innate immune cells: emerging therapeutic applications. *Ann Rheum Dis* **67**(Suppl 3), iii70–iii74.
- [34] Overman MJ, McDermott R, Leach JL, Lonardi S, Lenz HJ, Morse MA, Desai J, Hill A, Axelson M and Moss RA, et al (2017). Nivolumab in patients with metastatic DNA mismatch repair-deficient or microsatellite instability-high colorectal cancer (CheckMate 142): an open-label, multicentre, phase 2 study. *Lancet Oncol* **18**(9), 1182–1191.
- [35] Hewitt LC, Inam IZ, Saito Y, Yoshikawa T, Quaas A, Hoelscher A, Bollschweiler E, Fazzi GE, Melotte V and Langley RE, et al (2018). Epstein-Barr virus and mismatch repair deficiency status differ between oesophageal and gastric cancer: A large multi-centre study. *Eur J Cancer* **94**, 104–114.
- [36] Noble F, Mellows T, McCormick Matthews LH, Bateman AC, Harris S, Underwood TJ, Byrne JP, Bailey IS, Sharland DM and Kelly JJ, et al (2016). Tumour infiltrating lymphocytes correlate with improved survival in patients with oesophageal adenocarcinoma. *Cancer Immunol Immunother* **65**(6), 651–662.
- [37] Rauser S, Langer R, Tschernitz S, Gais P, Jutting U, Feith M, Hofler H and Walch A (2010). High number of CD45RO+ tumor infiltrating lymphocytes is an independent prognostic factor in non-metastasized (stage I-IIA) esophageal adenocarcinoma. *BMC Cancer* **10**, 608.
- [38] Zingg U, Montani M, Frey DM, Dirnhofner S, Esterman AJ, Went P and Oertli D (2010). Tumour-infiltrating lymphocytes and survival in patients with adenocarcinoma of the oesophagus. *Eur J Surg Oncol* **36**(7), 670–677.
- [39] Loeser H, Kraemer M, Gebauer F, Bruns C, Schroder W, Zander T, Persa OD, Alakus H, Hoelscher A and Buettner R, et al (2019). The expression of the immune checkpoint regulator VISTA correlates with improved overall survival in pT1/2 tumor stages in esophageal adenocarcinoma. *Oncimmunology* **8**(5), e1581546.
- [40] Schroder W, Holscher AH, Bludau M, Vallbohmer D, Bollschweiler E and Gutschow C (2010). Ivor-Lewis esophagectomy with and without laparoscopic conditioning of the gastric conduit. *World J Surg* **34**(4), 738–743.
- [41] Holscher AH, Schneider PM, Gutschow C and Schroder W (2007). Laparoscopic ischemic conditioning of the stomach for esophageal replacement. *Ann Surg* **245**(2), 241–246.
- [42] Messager M, Pasquer A, Duhamel A, Caranhac G, Piessen G, Mariette C and groupFRENCH Fw (2015). Laparoscopic Gastric Mobilization Reduces Postoperative Mortality After Esophageal Cancer Surgery: A French Nationwide Study. *Ann Surg* **262**(5), 817–822; discussion 22–23.
- [43] Mariette C, Markar SR, Dabakuyo-Yonli TS, Meunier B, Pezet D, Collet D, D'Journo XB, Brigand C, Perniceni T and Carrere N, et al (2019). Hybrid Minimally Invasive Esophagectomy for Esophageal Cancer. *N Engl J Med* **380**(2), 152–162.
- [44] Schneider PM, Metzger R, Schaefer H, Baumgarten F, Vallbohmer D, Brabender J, Wolfgarten E, Bollschweiler E, Baldus SE and Dienes HP, et al (2008). Response evaluation by endoscopy, rebiopsy, and endoscopic ultrasound does not accurately predict histopathologic regression after neoadjuvant chemoradiation for esophageal cancer. *Ann Surg* **248**(6), 902–908.
- [45] Simon R, Mirlacher M and Sauter G (2005). Tissue microarrays. *Methods Mol Med* **114**, 257–268.
- [46] Helbig D, Ihle MA, Putz K, Tantcheva-Poor I, Mauch C, Buttner R and Quaas A (2016). Oncogene and therapeutic target analyses in atypical fibroxanthomas and pleomorphic dermal sarcomas. *Oncotarget* **7**(16), 21763–21774.
- [47] Loeser H, Waldschmidt D, Kuetting F, Heydt C, Zander T, Plum P, Alakus H, Buettner R and Quaas A (2017). Copy-number variation and protein expression of DOT1L in pancreatic adenocarcinoma as a potential drug target. *Mol Clin Oncol* **6**(5), 639–642.
- [48] Valtorta E, Misale S, Sartore-Bianchi A, Nagtegaal ID, Paraf F, Lauricella C, Dimartino V, Hobor S, Jacobs B and Ercolani C, et al (2013). KRAS gene amplification in colorectal cancer and impact on response to EGFR-targeted therapy. *Int J Cancer* **133**(5), 1259–1265.
- [49] Fendri A, Khabir A, Mnejja W, Sellami-Boudawara T, Daoud J, Frikha M, Ghorbel A, Gargouri A and Mokdad-Gargouri R (2009). PIK3CA amplification is predictive of poor prognosis in Tunisian patients with nasopharyngeal carcinoma. *Cancer Sci* **100**(11), 2034–2039.
- [50] Kim JH, Lee JS, Kim EJ, Park KH, Kim KH, Yi SY, Kim HS, Cho YJ, Shin KH and Ahn JB, et al (2016). Prognostic implications of PIK3CA amplification in curatively resected liposarcoma. *Oncotarget* **7**(17), 24549–24558.
- [51] Holscher AH, Drebber U, Schmidt H and Bollschweiler E (2014). Prognostic classification of histopathologic response to neoadjuvant therapy in esophageal adenocarcinoma. *Ann Surg* **260**(5), 779–784; discussion 84–85.
- [52] Kim HS, Lee SE, Bae YS, Kim DJ, Lee CG, Hur J, Chung H, Park JC, Shin SK and Lee SK, et al (2016). PIK3CA amplification is associated with poor prognosis among patients with curatively resected esophageal squamous cell carcinoma. *Oncotarget* **7**(21), 30691–30701.
- [53] Shigaki H, Baba Y, Watanabe M, Murata A, Ishimoto T, Iwatsuki M, Iwagami S, Noshio K and Baba H (2013). PIK3CA mutation is associated with a favorable prognosis among patients with curatively resected esophageal squamous cell carcinoma. *Clin Cancer Res* **19**(9), 2451–2459.